

HIGHER-ORDER IMMERSED DISCONTINUOUS GALERKIN METHODS

SLIMANE ADJERID AND TAO LIN

Abstract. We propose new discontinuous finite element methods that can be applied to one-dimensional elliptic problems with discontinuous coefficients. These methods are based on a class of higher degree immersed finite element spaces and can be used with a mesh independent of the location of coefficient discontinuity. Numerical experiments are presented to show that these methods can achieve optimal convergence rates under both h and p refinements.

Key Words. immersed finite element, discontinuous Galerkin, discontinuous coefficient, interface problems

1. Introduction

It has been pointed out in the literature (for example, see [2]), that finite element methods should be designed/employed according to the problem to be solved. For boundary value problems (BVPs) with discontinuous coefficients, the conventional (including discontinuous Galerkin) finite element methods employ universal basis functions, but they have to be used with a mesh tailored in such a way that each element basically contains only one material [3, 5]. With this approach, it is difficult, if not impossible, to use uniform meshes, and the mesh has to be regenerated once the discontinuity has moved to a new location during a numerical simulation. The recently developed immersed finite element (IFE) methods [4, 9, 10, 11, 12, 14, 13] use an alternative approach in which the mesh can be independent of the coefficient discontinuity, but the basis functions are constructed according to the material interface and the jump conditions. The meshes are allowed to have elements containing the coefficient discontinuity interface. In other words, the interface is allowed to be immersed in these elements; hence, we call these methods the immersed finite element methods.

Higher degree finite element approximations for solutions to BVPs with enough smoothness can lead to exponential convergence rates and thus are very efficient. The discontinuous Galerkin (DG) finite element methods are flexible for implementing either local h or p refinements. The (DG) method

Received by the editors Received on March 1, 2007.

This article was partially supported by the National Science Foundation through the grants: DMS-0511806 and CMS-0427951.

was first used to solve the neutron equation [16] and was studied for initial-value problems for ordinary differential equations [1, 16]. Cockburn and Shu [7] extended the method to solve first-order hyperbolic partial differential equations of conservation laws. They also developed the Local Discontinuous Galerkin (LDG) method for convection-diffusion problems [8]. The reader can consult [6] for more information on DG methods.

However, mathematical models for many applications involving inhomogeneous materials yield nonsmooth solutions. Therefore, all the advantages of higher-order standard finite methods are lost unless the mesh is aligned with material discontinuities. Aligning the mesh with material interfaces may not be an obvious task and may lead to unnecessarily fine meshes in the presence, for instance, of thin multi-layer coatings and fibers. In this article, we present new and flexible higher degree finite element methods that combine features of IFE and DG methods for solving boundary value problems without requiring the mesh to be aligned with material interfaces. These methods can also achieve optimal convergence rates with respect to the polynomials employed.

It is known that the jump conditions can be used to uniquely define the linear IFE basis functions across a material interface [10, 11, 12, 13]. However, we have noticed that interface jump conditions are not enough to uniquely determine higher degree IFE basis functions. Improper choice of extra conditions to define higher degree IFE basis functions might lead to sub-optimal approximation capability [4]. The main goal of our article here is to present a class of extra conditions for unique determination of higher degree piecewise polynomial finite element basis functions that are able to optimally resolve the nonsmooth behavior of the solution across the interfaces without requiring the mesh to be aligned with the discontinuity.

This paper is organized as follows: In §2, we present two immersed discontinuous Galerkin finite element methods. In §3, we present a class of higher degree IFE spaces. In §4 we present several numerical results to demonstrate features of our new methods and conclude with a few remarks in §5.

2. Immersed discontinuous Galerkin methods

In this section we describe two immersed discontinuous Galerkin methods for a model boundary value problem on a domain $\Omega = (a, b)$: find u such that

$$(1) \quad (\sigma u')' = f, \quad a < x < b,$$

$$(2) \quad u(a) = u_a, \quad u(b) = u_b.$$

Without loss of generality, we assume that the domain $\Omega = (a, b)$ is separated into two sub-domains by an interface point $\alpha \in (a, b)$, across which the coefficient σ has a jump:

$$\sigma(x) = \begin{cases} \sigma^-, & x \in (a, \alpha), \\ \sigma^+, & x \in (\alpha, b). \end{cases}$$

At the interface α , we assume that the solution u satisfies the following jump conditions:

$$(3) \quad [u](\alpha) = 0, \quad [\sigma u'](\alpha) = 0,$$

where $[v](\alpha) = v(\alpha^+) - v(\alpha^-)$. We would like to point out that the results obtained here can be easily extended to cases in which σ has multiple discontinuity points.

First, we consider the immersed local discontinuous Galerkin (ILDG) method by introducing the auxiliary variable $q = \sigma u'$ and writing the model problem as a first-order system

$$(4a) \quad q' = f,$$

$$(4b) \quad \sigma u' = q, \quad a < x < b.$$

Let us introduce a partition of Ω : $\mathcal{T}_h : a = x_0 < x_1 < \dots < x_N = b$ without consideration of the interface location. Then, we multiply the first equation by a test function v and the second equation by w , integrate over a typical element $I_i = [x_i, x_{i+1}]$, $i = 0, 1, 2, \dots, N-1$, and apply integration by parts to obtain

$$(5a) \quad -qv|_{x_i}^{x_{i+1}} - (q, v')_{I_i} = (f, v)_{I_i},$$

$$(5b) \quad \begin{cases} \sigma uw|_{x_i}^{x_{i+1}} - [\sigma]uw(\alpha) - (\sigma u, w')_{I_i} = (q, w)_{I_i}, & \alpha \in I_i, \\ \sigma uw|_{x_i}^{x_{i+1}} - (\sigma u, w')_{I_i} = (q, w)_{I_i}, & \alpha \notin I_i. \end{cases}$$

We then use the local mixed weak form (5) to obtain a ILDG method by employing a standard discontinuous piecewise polynomial function space $S^{N,p}$ to approximate q and an immersed finite element (IFE) space $S_I^{N,p}$ to approximate u . Here

$$(6) \quad S^{N,p} = \{V \mid V|_{I_i} \in \mathcal{P}_p, i = 0, 1, \dots, N-1\},$$

and \mathcal{P}_p is the space of p -th degree polynomials. The IFE space $S_I^{N,p}$ is the set of piecewise polynomial functions that are formed by p -th degree polynomials on each element not containing an interface point, and by piecewise p -th degree polynomial functions on elements containing interfaces. The construction details for $S_I^{N,p}$ are presented in the next section.

Specifically, the ILDG method consists of finding $(U, Q) \in X^{N,p} = S_I^{N,p} \times S^{N,p}$ such that for all $(V, W) \in X^{N,p}$,

$$(7a) \quad \hat{Q}V|_{x_i}^{x_{i+1}} + (Q, V')_{I_i} = (f, V)_{I_i},$$

$$(7b) \quad \begin{cases} \sigma \hat{U}W|_{x_i}^{x_{i+1}} - (\sigma U, W')_{I_i} = (Q, W)_{I_i}, & \alpha \notin I_i, \\ \sigma \hat{U}W|_{x_i}^{x_{i+1}} - [\sigma](\alpha)(UW)(\alpha) - (\sigma U, W')_{I_i} = (Q, W)_{I_i}, & \alpha \in I_i. \end{cases}$$

The ILDG method is completed by using the following numerical fluxes for the minimum diffusion LDG method introduced by Cockburn *et al.* [8]:

$$(8a) \quad \hat{U}(x_i) = U(x_i^-), \quad \hat{Q}(x_i) = Q(x_i^+), \quad i = 1, 2, \dots, N-1.$$

Fluxes at boundary points are given by the boundary condition as follows

$$(8b) \quad \begin{aligned} \hat{U}(a) &= u(a) & \hat{Q}(a) &= Q(a^+), \\ \hat{U}(b) &= u(b) & \hat{Q}(b) &= Q(b^-) - \frac{p}{h}(u(b) - U(b^-)). \end{aligned}$$

Next, we consider the immersed discontinuous Galerkin (IDG) method based on the DG method proposed by Riviere *et al.* [15] which consists of determining $U \in S_I^{N,p}$ such that

$$(9a) \quad \mathcal{A}(U, V) = L(V), \quad \forall V \in S_I^{N,p}.$$

where

$$(9b) \quad \begin{aligned} \mathcal{A}(U, V) &= \sum_{i=0}^{N-1} (\sigma U', V')_{I_i} + \sum_{i=1}^{N-1} (\{\sigma U'\}[V] - \{\sigma V'\}[U] + \gamma[U][V]) (x_i) \\ &\quad - U(0^+) (\sigma V'(0^+) - \gamma V(0^+)) + \sigma U'(0^+) V(0^+) \\ &\quad + U(1^-) (\sigma V'(1^-) - \gamma V(1^-)) - \sigma U'(1^-) V(1^-), \end{aligned}$$

and

$$(9c) \quad L(V) = (f, V)_\Omega - u_0 (\sigma V'(0^+) - \gamma V(0^+)) + u_1 (\sigma V'(1^-) - \gamma V(1^-)).$$

Here we select $\gamma = 1/h$.

3. A class of higher degree IFE basis functions

In this section, we construct the basis functions for the finite element spaces $S^{N,p}$ and $S_I^{N,p}$. Because of the discontinuous formulation, we only need to define these spaces locally on a typical element I_i , $i = 0, 1, \dots, N-1$. As usual, we can just construct related spaces on the reference element $\hat{I} = [-1, 1]$, then define those spaces on I_i by the usual affine transformation.

First, let us recall the standard hierarchical shape functions on the reference element \hat{I} . The first two linear basis functions are

$$(10a) \quad \hat{\phi}_0(t) = (1-t)/2, \quad \hat{\phi}_1(t) = (t+1)/2, \quad t \in \hat{I}.$$

The higher degree shape functions are defined by Lobatto polynomials as

$$(10b) \quad \hat{\phi}_k(t) = c_k (P_k(t) - P_{k-2}(t)), \quad k = 2, \dots, p, \quad t \in \hat{I},$$

where c_k is a scaling factor that may be determined by normalizing the basis. Then, we can use

$$\hat{\mathcal{P}}_p = \text{span}\{\hat{\phi}_i(t), i = 0, 1, \dots, p\}$$

to define the local spaces on a non-interface element for both $S^{N,p}$ and $S_I^{N,p}$.

On an interface element, we define the local space with piecewise p -th degree polynomial functions satisfying the interface jump conditions as the minimum requirement. However, for $p \geq 2$, extra conditions should be carefully added; otherwise the space defined may not have the optimal approximation capability [4]. We now propose to construct the local space on

an interface element such that its functions can match the smoothness of the exact solution across the interface. We can implement this idea hierarchically as follows. Without loss of generality, we assume that $\hat{I} = [-1, 1]$ contains one interface $\hat{\alpha} \in (-1, 1)$.

Two linear IFE basis functions [10]:

$$\hat{\phi}_i^I(x) = \begin{cases} a_{i1}t + b_{i1}, & -1 \leq t \leq \hat{\alpha}, \\ a_{i2}t + b_{i2}, & \hat{\alpha} \leq t \leq 1, \end{cases}$$

$$\hat{\phi}_0^I(-1) = 1, \hat{\phi}_0^I(1) = 0, \hat{\phi}_1^I(-1) = 0, \hat{\phi}_1^I(1) = 1,$$

$$[\hat{\phi}_i^I](\hat{\alpha}) = 0, [\sigma(\hat{\phi}_i^I)]'(\hat{\alpha}) = 0, i = 0, 1.$$

A quadratic IFE basis function:

$$\hat{\phi}_2^I(t) = \begin{cases} (t + 1)(a_{21}t + b_{21}), & -1 \leq t \leq \hat{\alpha}, \\ (t - 1)(a_{22}t + b_{22}), & \hat{\alpha} \leq t \leq 1, \end{cases}$$

$$[\hat{\phi}_2^I](\hat{\alpha}) = 0, [\sigma(\hat{\phi}_2^I)]'(\hat{\alpha}) = 0, [\sigma(\hat{\phi}_2^I)]''(\hat{\alpha}) = 0$$

Setting $a_{22} = 1$ uniquely determines $\hat{\phi}_2^I(t)$. Also, we note that $\langle \hat{\phi}_2^I, \hat{\phi}_1^I \rangle_{\hat{I}} = 0$, where $\langle f, g \rangle = \int_{-1}^{\hat{\alpha}} \sigma^- f' g' dx + \int_{\hat{\alpha}}^1 \sigma^+ f' g' dx$.

The p^{th} - degree IFE shape function:

$$\hat{\phi}_p^I(t) = \begin{cases} (t + 1) \left(\sum_{i=0}^{p-1} a_{p,i}^1 t^i \right), & -1 \leq t \leq \hat{\alpha}, \\ (t - 1) \left(\sum_{i=0}^{p-1} a_{p,i}^2 t^i \right), & \hat{\alpha} \leq t \leq 1, \end{cases}$$

$$[\hat{\phi}_p^I](\hat{\alpha}) = 0, [\sigma(\hat{\phi}_p^I)]^{(k)}(\hat{\alpha}) = 0, k = 1, 2, \dots, p,$$

$$\langle \hat{\phi}_p^I(t), \hat{\phi}_k^I(t) \rangle_{\hat{I}} = 0, k = 2, 3, \dots, p - 1.$$

Setting $a_{p,2}^2 = 1$ uniquely determines $\hat{\phi}_p^I(t)$. This coefficient can also be determined by normalizing these shape functions. Figures 1-3 illustrate the difference between the IFE basis functions and the standard Lobatto hierarchical basis functions.

Finally, we let

$$\hat{\mathcal{P}}_p^I = span\{\hat{\phi}_i^I, i = 0, 1, \dots, p\},$$

and use it to form the local space for $S_I^{N,p}$ on an interface element via the usual affine transformation.

Remarks:

- (1) If $\hat{\alpha} = \pm 1$ or σ is continuous at the interface $t = \hat{\alpha}$, then $\hat{\phi}_i^I, i = 0, 1, \dots$ reduces to the standard Lobatto hierarchical basis functions.
- (2) All immersed basis functions satisfy $[\sigma\phi^{(k)}](\alpha) = 0, k \geq 1$.

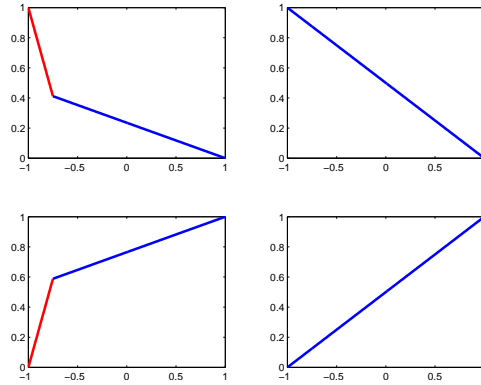


FIGURE 1. The 1st degree IFE (left) and standard (right) basis functions.

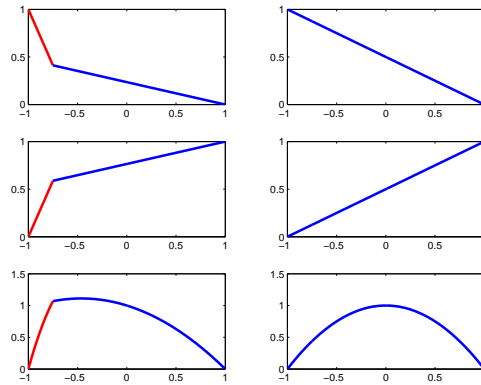


FIGURE 2. The 2nd degree IFE (left) and standard (right) basis functions.

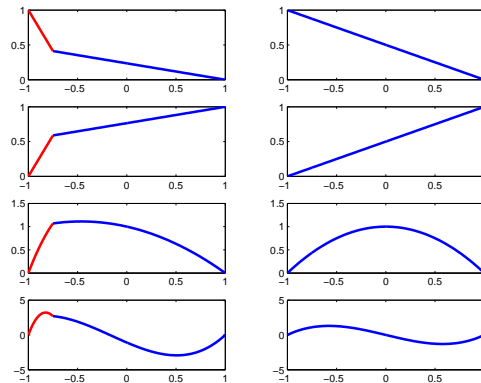


FIGURE 3. The 3rd degree IFE (left) and standard (right) basis functions.

- (3) The construction procedure can be easily extended to handle the case in which the interface element contains multiple interfaces.
- (4) One can also construct Lagrange type IFE basis functions using the same smoothness conditions. Details and related error estimations will be reported in another article.

4. Numerical Examples

In this section we present numerical examples to demonstrate the features of IFE spaces and the immersed DG methods, especially their optimal approximation capability.

4.1. Approximation capability of higher degree IFE spaces.

Example 1: We use this example to demonstrate the accuracy of the IFE interpolation of the following function:

$$(11) \quad u(x) = \begin{cases} e^x, & x \in [0, \alpha), \\ \left[(x - \alpha)^m + \frac{\sigma^-}{\sigma^+} \right] e^x + \left(1 - \frac{\sigma^-}{\sigma^+} \right) e^\alpha, & x \in (\alpha, 1] \end{cases}$$

where we always choose $m = p+1$ with p being the degree of the polynomials used our finite element methods.

We can show that

$$[u](\alpha) = 0, \quad [\sigma u^{(k)}](\alpha) = 0, \quad k = 1, 2, \dots, m-1, \quad [\sigma u^{(m)}](\alpha) \neq 0.$$

We interpolate u by the 2nd and 3rd degree hierarchical IFE functions and presents the \mathcal{L}^2 and \mathcal{H}^1 errors in Table 1. The data in this table obeys the following relation

$$\|u - I_h u\|_k \leq Ch^{p+1-k}, \quad k = 0, 1$$

where $I_h u$ is the p -th degree IFE interpolation of u which indicates that these IFE spaces have the optimal approximation capability according to the polynomials employed in these spaces.

4.2. Examples for the ILDG method.

Example 2: We consider the model interface problem (1) with one interface

$$(12a) \quad (\sigma u')' = e^x, \quad 0 < x < 4,$$

where

$$(12b) \quad \sigma = \begin{cases} 2, & 0 \leq x < 1 \\ 50, & 1 \leq x \leq 4, \end{cases}$$

subject to the boundary conditions $u(0) = -2$, $u(4) = 10$. We solve this problem using the ILDG method on uniform meshes having $N = 11, 13, 15, 17$ elements and $p = 1, 2, 3, 4, 5$. The the \mathcal{L}^2 errors in u and q are presented in

N	2nd degree IFE error		3rd degree IFE error	
	\mathcal{L}^2 norm	\mathcal{H}^1 norm	\mathcal{L}^2 norm	\mathcal{H}^1 norm
20	8.3737e-6	1.0859e-3	1.8702e-7	3.7422e-5
30	2.4965e-6	4.8548e-4	3.6017e-8	1.0803e-5
40	1.0556e-6	2.7369e-4	1.1403e-8	4.5613e-6
50	5.4106e-7	1.7534e-4	4.7768e-9	2.4589e-6
60	3.1329e-7	1.2183e-4	2.2809e-9	1.3682e-6
70	1.9735e-7	8.9531e-5	1.2168e-9	8.5141e-7
rate	2.9919	1.9923	4.0078	3.0033

TABLE 1. Errors of the 2nd and 3rd degree hierarchical IFE interpolations. N is the number uniform elements used in the interpolation. $\alpha = \pi/6$, $\sigma^- = 1$, $\sigma^+ = 20$.

N	$p = 1$	$p = 2$	$p = 3$	$p = 4$	$p = 5$
	$\ u - U\ $				
11	0.12439	0.0035	7.6757e-5	1.3662e-6	2.0431e-8
13	0.70939	0.001691	3.13555e-5	4.7346e-7	5.98157e-9
15	0.043769	9.043e-4	1.45366e-5	1.8961e-7	2.08108e-9
17	0.028585	5.21922e-4	7.3917 e-6	8.5526e-8	8.25496e-10
rate	3.37	4.37	5.37	6.36	7.37
	$\ q - Q\ $				
11	0.30322	0.89059e-2	0.19916e-3	3.5817e-6	5.4152e-8
13	0.21786	0.54197e-2	0.10215e-3	1.5711e-6	1.9952e-8
15	0.16463	0.35411e-2	0.58034e-4	7.6485e-7	8.4752e-9
17	0.12825	0.24363e-2	0.35107e-4	4.1265e-7	4.01 e-9
rate	1.97	2.97	3.98	4.97	5.97

TABLE 2. Errors $\|u - U\|$ and $\|q - Q\|$ on uniform meshes having $N = 11, 13, 15, 17$ elements and $p = 1, 2, 3, 4, 5$ for Example 2.

Table 2. These results indicate that $\|u - U\|$ and $\|q - Q\|$ converge to 0 at $O(h^{p+2})$ and $O(h^{p+1})$ rates, respectively, under h -refinement. We observe an $O(h^{p+2})$ superconvergence result for u . Next, we solve the problem with $N = 11, 21, 31$ and $p = 1$ to 5 and plot the \mathcal{L}^2 error versus degrees of freedom in Figure 4, from which we can see that the errors behave the same way as for analytical solutions, *i.e.*, they converge exponentially fast under p refinement.

Example 3: We now demonstrate that our IFE methods can perform optimally even if some of the interface element contain multiple interfaces.

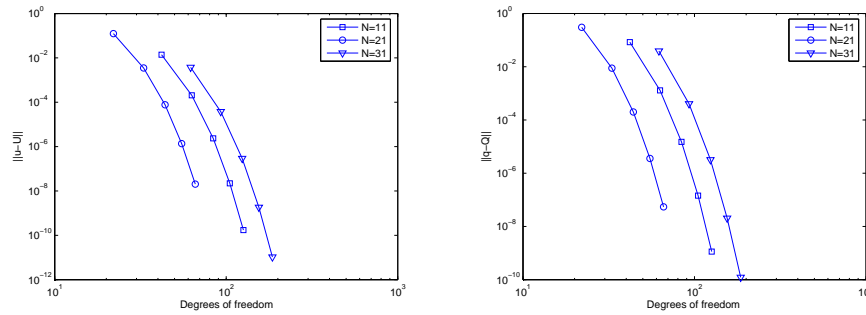


FIGURE 4. Errors $\|u - U\|$ (left) and $\|q - Q\|$ (right) versus number of degrees of freedom for Example 2 using uniform meshes having $N = 11, 21, 31$ elements and $p = 1$ to 5.

Consider the model problem (1) with three interfaces configured as follows:

$$(13) \quad \sigma = \begin{cases} -2, & 0 \leq x < \sqrt{2} \\ -10, & \sqrt{2} \leq x < \sqrt{5} \\ -1, & \sqrt{5} \leq x < \sqrt{5} + 0.002 \\ -10, & \sqrt{5} + 0.002 \leq x \leq 4 \end{cases}$$

We apply the Dirichlet boundary conditions $u(0) = -2$ and $u(4) = 5$ and solve the model problem using the ILDG on uniform meshes having $N = 15, 20, 25, 30, 35, 45$ elements and $p = 1$ to 4. Each of the meshes generated with these N always contains one element with two interfaces. The \mathcal{L}^2 errors for u and q versus N are plotted in Figure 5. The numerical results suggest $O(h^{p+1.75})$ and $O(h^{p+1})$ convergence rates in the \mathcal{L}^2 for u and q , respectively, under mesh refinement. We also plot the errors versus the number of degrees of freedom in Figure 6 to demonstrate the exponential converge rates under p refinement.

Example 4: In this example we show that our IFE DG methods has the capability to handle boundary layer problems in which the interface α approaches the boundary. We consider the linear diffusion problem (1) with one interface

$$(14a) \quad -(\sigma u')' = e^x, \quad 0 < x < 4,$$

where

$$(14b) \quad \sigma = \begin{cases} 1, & 0 \leq x < \alpha \\ 190, & \alpha \leq x \leq 4, \end{cases}$$

subject to the boundary conditions $u(0) = 0, u(4) = 4$. We solve a set of interface problems with $\alpha = 0.05, 0.03, 0.01, 0.001, 0.0001$ using the ILDG method on uniform meshes having $N = 20, 30, 40, 50, 60, 70$ elements and

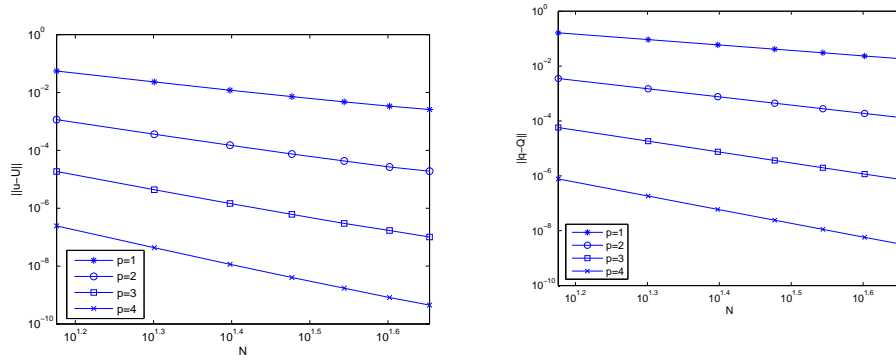


FIGURE 5. \mathcal{L}^2 errors $\|u - U\|$ (left) and $\|q - Q\|$ (right) for Example 3 using uniform meshes having $N = 15, 20, 25, 30, 35, 40, 45$ elements and $p = 1$ to 4.

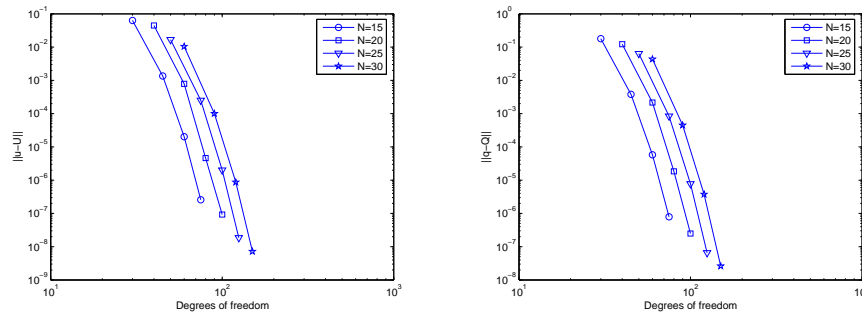


FIGURE 6. \mathcal{L}^2 errors $\|u - U\|$ (left) and $\|q - Q\|$ (right) versus the number of the degrees of freedom for Example 3 using uniform meshes having $N = 15, 20, 25, 30$ elements and $p = 1$ to 4.

$p = 3$. We present the \mathcal{L}^2 errors $\|u - U\|$ and $\|q - Q\|$ in Table 3 and 4, respectively, with their convergence rates. These results show superconvergence rates for u and optimal convergence rates for q independent of the interface position.

4.3. Examples for the IDG method.

N	$\alpha = 5.e - 2$	$\alpha = 3.e - 2$	$\alpha = 1.e - 2$	$\alpha = 1.e - 3$	$\alpha = 1.e - 4$
20	3.2277e-6	3.2259e-6	3.2372e-6	3.2282e-6	3.4089e-6
30	3.6182e-7	3.6183e-7	3.6414e-7	3.6121e-7	3.9746e-7
40	7.6116e-8	7.6784e-8	7.6617e-8	7.6079e-8	8.7113e-8
50	2.2956e-8	2.3009e-8	2.2773e-8	2.2778e-8	2.6984e-8
60	8.7780e-9	8.5008e-9	8.4816e-9	8.5650e-9	1.0394e-8
70	3.9017e-9	3.7186e-9	3.7276e-9	3.7929e-9	4.6502e-9
rate	5.36	5.4	5.4	5.39	5.27

TABLE 3. Errors $\|u-U\|$ and their convergence rates on uniform meshes having $N = 20, 30, 40, 50, 60, 70$ elements and $p = 3$ for Example 4 with $\alpha = 0.05, 0.03, 0.01, 0.001, 0.0001$.

N	$\alpha = 5.e - 2$	$\alpha = 3.e - 2$	$\alpha = 1.e - 2$	$\alpha = 1.e - 3$	$\alpha = 1.e - 4$
20	2.0082e-5	1.8369e-5	2.8913e-5	2.0956e-5	9.2505e-5
30	3.9944e-6	4.0545e-6	5.2925e-6	3.6866e-6	1.4134e-5
40	1.1582e-6	1.4292e-6	1.3772e-6	1.1578e-6	3.6784e-6
50	5.3142e-7	5.5469e-7	4.8860e-7	4.9071e-7	1.2874e-6
60	2.8380e-7	2.3197e-7	2.2870e-7	2.4908e-7	5.4489e-7
70	1.5106e-7	1.2755e-7	1.3022e-7	1.4242e-7	2.6333e-7
rate	3.89	3.98	4.38	3.98	4.68

TABLE 4. Errors $\|q-Q\|$ and their convergence rates on uniform meshes having $N = 20, 30, 40, 50, 60, 70$ elements and $p = 3$ for Example 4 with $\alpha = 0.05, 0.03, 0.01, 0.001, 0.0001$.

Example 5. This example is used to demonstrate the performance of IDG method applied to solve the model interface problem (1) whose exact solution is given by (11) with

$$\sigma = \begin{cases} 1, & x \in (0, \pi/6), \\ 20, & x \in (\pi/6, 1). \end{cases}$$

The errors in both \mathcal{L}^2 and \mathcal{H}^1 norms for $p = 2, 3$ are presented in Table 5 from which we can see that the IDG solution has the optimal convergence rate in both \mathcal{L}^2 and \mathcal{H}^1 norms for odd polynomial degree. For even degree, the IDG solution still has the optimal convergence rate in \mathcal{H}^1 norm, but not in \mathcal{L}^2 norm. However, this is not the limitation of the immersed finite element because similar behavior is also observed for this particular DG method used with standard finite element for BVPs with continuous coefficients[15].

Example 6: We use this example to show that the IFE DG methods proposed here can use one mesh to solve a sequence of BVPs whose interfaces vary from one to the next. To be specific, we apply the 3rd degree IDG method to a set of model boundary problems (1) whose exact solution are given

N	2nd degree IFE error		3rd degree IFE error	
	\mathcal{L}^2 norm	\mathcal{H}^1 norm	\mathcal{L}^2 norm	\mathcal{H}^1 norm
20	3.0554e-3	7.9530e-3	1.9363e-6	4.1140e-5
30	1.3134e-3	3.3730e-3	3.8886e-7	1.1566e-5
40	7.2907e-4	1.8741e-3	1.2033e-7	4.8068e-6
50	4.6676e-4	1.2067e-3	4.7826e-8	2.5343e-6
60	3.2368e-4	8.4028e-4	2.3484e-8	1.4052e-6
70	2.3583e-4	6.0938e-4	1.3012e-8	8.7131e-7
rate	2.0682	2.0873	4.0050	3.0995

TABLE 5. The IDG errors for $p = 2, 3$ on uniform meshes having $N = 20, 30, 40, 50, 60, 70$ elements for Example 5 with $\alpha = \pi/6$, $\sigma^- = 1, \sigma^+ = 20$.

by (11), but whose interface α converge to 0.5. The errors of the IDG solutions for these BVPs are presented in Tables 6 and 7. On the same set of meshes, our IDG method shows a similar convergence behavior for all interface locations. We believe that this is a useful feature for design problems in which the location of material interfaces need to be determined optimally.

α	0.5063	0.5031	0.5021	0.5016	0.5013	0.5010
N=20	1.99e-6	2.00e-6	2.02e-6	2.03e-6	2.04e-6	2.04e-6
N=30	3.90e-7	3.91e-7	3.93e-7	3.96e-7	3.99e-7	4.00e-7
N=40	1.23e-7	1.23e-7	1.24e-7	1.24e-7	1.25e-7	1.26e-7
N=50	5.07e-8	5.05e-8	5.05e-8	5.06e-8	5.09e-8	5.11e-8
N=60	2.45e-8	2.43e-8	2.43e-8	2.44e-8	2.44e-8	2.45e-8
N=70	1.33e-8	1.31e-8	1.31e-8	1.31e-8	1.31e-8	1.32e-8
rate	3.9974	4.0113	4.0192	4.0254	4.0275	4.0269

TABLE 6. IDG \mathcal{L}^2 errors using $p = 3$ on uniform meshes having $N = 20, 30, 40, 50, 60, 70$ elements for Example 6 with a sequence of $\alpha_k \rightarrow 0.5$ and $\sigma^- = 1, \sigma^+ = 20$.

5. Conclusions

In this manuscript we developed new higher-order finite element methods that combine features of discontinuous Galerkin and immersed finite element methods to solve boundary value problems with discontinuous coefficients. The proposed methods can use a mesh independent of the location of discontinuity, if desired, even a uniform mesh can be used. The proposed methods have the flexibility of DG methods for both h and p refinement. The higher degree immersed finite element spaces introduced in this manuscript have

α	0.5063	0.5031	0.5021	0.5016	0.5013	0.5010
N=20	4.55e-5	4.35e-5	4.29e-5	4.28e-5	4.28e-5	4.27e-5
N=30	1.28e-5	1.26e-5	1.24e-5	1.23e-5	1.23e-5	1.23e-5
N=40	5.15e-6	5.25e-6	5.16e-6	5.12e-6	5.09e-6	5.08e-6
N=50	2.57e-6	2.65e-6	2.62e-6	2.50e-6	2.58e-6	2.58e-6
N=60	1.46e-6	1.51e-6	1.51e-6	1.50e-6	1.49e-6	1.48e-6
N=70	9.14e-7	9.36e-7	9.44e-7	9.39e-7	9.33e-7	9.30e-7
rate	3.1243	3.0623	3.0456	3.0481	3.0523	3.0555

TABLE 7. IDG \mathcal{H}^1 errors using $p = 3$ on uniform meshes having $N = 20, 30, 40, 50, 60, 70$ elements for Example 6 with a sequence of $\alpha_k \rightarrow 0.5$ and $\sigma^- = 1, \sigma^+ = 20$.

been demonstrated to have the optimal approximation capability with respect to the degree of polynomials employed. It is in our plan to extend these immersed discontinuous Galerkin methods to systems of partial differential equations with discontinuous coefficients used to model composite materials in two and three dimensions.

References

- [1] S. Adjerid, K. D. Devine, J. E. Flaherty, and L. Krivodonova. A posteriori error estimation for discontinuous Galerkin solutions of hyperbolic problems. *Computer Methods in Applied Mechanics and Engineering*, 191:1097–1112, 2002.
- [2] I. Babuška and J. Osborn. Generalized finite element methods: their performance and relation to mixed methods. *SIAM J. Numer. Anal.*, 20(3):510–536, 1983.
- [3] J. Bramble and J. King. A finite element method for interface problems in domains with smooth boundary and interfaces. *Adv. Comput. Math.*, 6:109–138, 1996.
- [4] B. Camp, T. Lin, Y. Lin, and W.W.Sun. Quadratic immersed finite element spaces and their approximation capabilities. *Advances in Computational Mathematics*, 24:81–112, 2006.
- [5] Z. Chen and J. Zou. Finite element methods and their convergence for elliptic and parabolic interface problems. *Numer. Math.*, 79:175–202, 1998.
- [6] B. Cockburn, G. E. Karniadakis, and C. W. Shu, editors. *Discontinuous Galerkin Methods Theory, Computation and Applications, Lectures Notes in Computational Science and Engineering*, volume 11. Springer, Berlin, 2000.
- [7] B. Cockburn and C. W. Shu. TVB Runge-Kutta local projection discontinuous Galerkin methods for scalar conservation laws II: General framework. *Mathematics of Computation*, 52:411–435, 1989.
- [8] B. Cockburn and C. W. Shu. The local discontinuous Galerkin finite element method for convection-diffusion systems. *SIAM Journal on Numerical Analysis*, 35:2240–2463, 1998.
- [9] R. Ewing, Z. Li, T. Lin, and Y. Lin. The immersed finite volume element method for the elliptic interface problems. *Mathematics and Computers in Simulation*, 50:63–76, 1999.
- [10] Z. Li. The immersed interface method using a finite element formulation. *Applied Numer. Math.*, 27:253–267, 1998.
- [11] Z. Li, T. Lin, Y. Lin, and R. Rogers. An immersed finite element space and its approximation capability. *Numerical Methods for Partial Differential Equations*, 20(3):338–367, 2004.

- [12] Z. Li, T. Lin, and X. Wu. New cartesian grid methods for interface problems using finite element formulation. *Numerische Mathematik*, 96(1):61–98, 2003.
- [13] T. Lin, Y. Lin, R. Kafafy, and J. Wang. 3-d immersed finite element methods for electric field simulation in composite materials. *International Journal for Numerical Methods in Engineering*, 64:904–972, 2005.
- [14] T. Lin, Y. Lin, R. Rogers, and L. Ryan. A rectangular immersed finite element method for interface problems. In P. Minev and Y. Lin, editors, *Advances in Computation: Theory and Practice, Vol. 7*, pages 107–114. Nova Science Publishers, Inc., 2001.
- [15] B. Riviere, M. Wheeler, and V. Girault. Improved energy estimates for interior penalty, constrained and discontinuous Galerkin methods for elliptic problems. part i. *Comput. Geosci.*, 3:337–360, 1999.
- [16] P. L. Saint and P. Raviart. On a finite element method for solving the neutron transport equations. In C. de Boor, editor, *Mathematical Aspects of Finite Elements in Partial Differential Equations*, pages 89–145, New York, 1974. Academic Press.

Department of Mathematics, Virginia Polytechnic Institute and State University, Blacksburg, VA 24061-0123

E-mail: adjerids@math.vt.edu, tlin@math.vt.edu